

Experimental investigations on mechanical and tribological behavior of AA7075 reinforced with ceramic particles

B. Thamarai Kannan^{a,*}, A. Sagai Francis Britto^b, S. Senthilraja^c and R. Rajkumar^d

^aKPR Institute of Engineering and Technology, Arasur, Coimbatore, Tamil Nadu, India

^bRohini College of Engineering & Technology, Palkulam, Tamil Nadu, India

^cSRM Institute of Science and Technology, Kattankulathur, Trichy, Tamil Nadu, India

^dKongu Engineering College, Erode, Tamil Nadu, India

Fly ash coal combustion dust from thermal power plants is one of the world's largest non-hazardous solid wastes. Effective utilization of fly ash as a secondary reinforcement in metal matrix composites significantly enhances properties and is highly appreciable for waste management systems. Present experimental scrutiny primarily spotlights on the mechanical, morphology, and wear behaviour of AA7075/Fly ash composites. The stir casting technique with regular feeding method was utilized for the fabrication of 4 wt.%, 8 wt.%, 12 wt.%, 16 wt.%, and 20 wt.% fly ash reinforced AMFAR (Aluminum matrix fly ash reinforced composites). Tensile, hardness, and low velocity impact behaviour of the samples, along with the sliding wear and morphology analysis, were carried out to study the material behaviour under different operational conditions. The results show that fly ash as a secondary reinforcement improves the mechanical performance of the samples significantly. At the same time, 20 wt.% fly ash content exhibits better mechanical, wear performance and reasonable particle distribution. The proposed hybrid composites are preferred for high-strength automobile applications as well as their industrial machine counterparts.

Keywords: AA7075, Stir casting, Hardness, Sliding wear, Wear rate.

Introduction

Numerous classes of aluminium alloys are commercially utilized by various engineering domains at the same time. Day-by-day, new materials are also established in the engineering industry. These newly developed materials are effectively used in automotive, marine, aircraft, and spacecraft applications due to their lightweight, durability, shape-memory nature, and high strength [1]. India is the third largest coal production country in the world with almost 120-150 million tonnes of coal-based fly ash waste derived from the power plants around the country every year [2]. Frictional, wear behavior prediction, and strength improvement of advanced composites are always difficult tasks. This phenomenon was addressed by introducing discontinuously reinforced foam or filler materials into the matrix [3, 4]. Modern automotive industries prefer low-cost materials, easy manufacturing techniques, high thickness, and lightweight emergent materials in order to utilize for robotic machines [5]. The composite is in the form of particles, i.e., oxides like SiC, boride oxide, ceramic, ferrous oxide, and aluminum oxides, which are the most commonly used

secondary reinforcements in aluminium composites. Based on the strength and stiffness requirements of end products, small percentages of reinforcements were included to discover high-strength friction-resistant composites [6, 7].

Diverse researchers from around the world experimented with various filler and matrix materials in order to improve the wear behavior of composites. Reddappa et al. [8] utilized the stir casting route to prepare AA 6061-beryl composites with four different wt.% of beryl fillers. Pin-on-disc sliding wear tests were performed with a load range of 5N to 15N and a sliding speed of 1.66 m/s for a dissimilar sliding distance of 1 km to 6 km, and excellent results were obtained at 10% beryl with minimal wear loss of fabricated material. Umanath et al. [9] prepared aluminium-base (AA6061) hybrid composite materials reinforced with SiC and Al₂O₃ particulate matter. The results showed that increasing the volume content of reinforcements reduced wear rate. The wear rates and frictional coefficients of hybrid composites are smaller in comparison to the individual composites and the matrix alloy. While improving the volume content of reinforcements, there is an improvement in the micro hardness of the composite along with porosity also observed. Balu Mahandiran [10] used stir casting to create AA6061/SiC composites with filler additions of 10 and 15% by weight. Complete experiments were

*Corresponding author:
Tel : +91 7339266800
E-mail: thamarai kannan254@gmail.com

designed using the Taguchi optimization technique. Confirmation results clearly show that there is a very small error deviation between experimental and optimal values. Mishra [11] used a conventional liquid casting technique to create a composite material with varying Al_2O_3 content. The graphical and methodical findings of Taguchi's optimal process parameters for 10N of load and 400 m of sliding distance possess very minimal wear mass loss in 6 wt.% of Al_2O_3 filled composites. Natarajan [12] developed low-cost Al 6063/TiB2 by the combination of K_2TiF_6 and KBF_4 with melted alloy. These in situ formulated composite materials are distinguished through micro hardness analysis, X-ray diffract meter, and scanning electron microscope results reveal that wear rate declines with the increasing weight percent of TiB2, at the same time it rises with an improvement in applied load. Babu Rao [13] used a stir casting procedure to create an AA2024 alloy reinforced with 5% fly ash. The composite has demonstrated excellent resistance to wear when compared to the base alloy with respect to the lowest applied loads. The wear characteristics of dissimilar materials like steel, aluminum, and brass were examined by Hani Aziz Ameen [14] by conducting dry sliding wear tests at different loads, sliding velocity, and time with fixed distance. A Square mathematics model was established to examine the wear rate over various deadlines with respect to varying sliding velocity. The findings reveal that the adhesion wear rate would be directly proportionate with load, sliding velocity, and time. There is a very low wear rate observed in carbon steel compared to other similar grade materials. In friction stir welded aluminum (Al 6063) matrix composites, Suresh Babu et al. investigated the effect of reinforcing particles on the mechanical characteristics of the metal matrix composition. For hybrid composites with a 20% weight proportion of reinforced material, the ideal friction stir weld settings were found [15]. The impact of nano aluminum nitride (AlN) on the mechanical characteristics and microstructure of vitrified bond diamond tools has been studied by Kuan-Hong Lin et al. More over 20 vol% of nano AlN would promote gas eruption from the matrix during the sintering process, resulting in a greater number of pores and expanding vitrified matrix. The mechanical characteristics of vitrified bond diamond

tools were reduced by the degraded microstructure [16]. By using a hot press to sinter SiC-TiC composites with aluminum and yttrium nitrate additive, Sung et al. investigated the sintered body's crystal phase, relative density, microstructure, electrical resistivity, and mechanical characteristics [17]. The present work aims to improve mechanical and wear behavior and conduct micro structural studies on Al-fly ash reinforced composites to compare hybrid configurations with pure aluminium.

Materials and Methods

Materials

The aluminum composition includes 99.9277% of pure aluminium and a remaining small amount of Mg, Si, Fe, Cu, Mn, etc. The detailed percentage of compositions is shown in Table 1. Fly ash was collected from the Mettur Thermal Power Station. It's a coal-fired electric power station located in Mettur, Tamilnadu. Table 2 shows the detailed chemical composition of the as-received fly ash percentages. The average particle size of fly ash is about 10 μm .

Fabrication of hybrid composites

The composites were prepared by the liquid state stir casting method. Stir casting is one of the most cost-effective and relatively simplest methods for producing metal matrix composites. First of all, the commercially available premeasured quantity of pure aluminium (AA7075) metal was melted and cast by an electrical resistance furnace in a graphite crucible. Then aluminium billets (unreinforced) and hybrid aluminium composite samples were prepared with five different

Table 3. shows the percentages of reinforcement for test samples.

Sample code	Composition of samples
Sample 1 (Neat)	Aluminium alloy (AA7075)
Sample 2 (HC1)	AA7075 + 4 wt.% Fly ash
Sample 3 (HC2)	AA7075 + 8 wt.% Fly ash
Sample 4 (HC3)	AA7075 + 12 wt.% Fly ash
Sample 5 (HC4)	AA7075 + 16 wt.% Fly ash
Sample 6 (HC5)	AA7075 + 20 wt.% Fly ash

Table 1. Chemical composition of AA7075 as received (in weight%).

Element	Al	Mg	Si	Fe	Cu	Mn	Cl
wt.%	99.9277	0.017	0.022	0.0012	0.0001	0.024	0.004

Table 2. Chemical composition of as-received fly ash (in weight percentages).

Element	SiO_2	Al_2O_3	Fe_2O_3	CaO	MnO_2	K_2O	TiO_2	LOI
wt.%	50.5	22.54	7.3	5.1	1.0	0.5	0.35	Balance

fly ash reinforcement percentages, as shown in Table 3 such as 4 wt.%, 8 wt.%, 12 wt.%, 16 wt.%, and 20 wt.%. The high purity aluminium (99.93%) was melted in a graphite crucible using electrical resistance heating at 750 °C. The fly ash particles were preheated up to 300 °C to remove the moisture content for two hours. The fly ash particles were added at the time of formation of vortex due to stirring process in the melt. The weight percentage of 4 wt.%, 8 wt.%, 12 wt.%, 16 wt.%, and 20 wt.% of fly ash was added into the aluminium matrix under the protected inert atmosphere of argon gas.

The steel impeller was used to properly distribute the preheated fly ash reinforcement with matrix material. The impeller rotates at a speed of 750 rpm and stirring was carried out continuously for 3-5 minutes after the addition of fly ash filler reinforcement in the matrix. Then, immediately the molten metal was poured into a 300 °C preheated mould to obtain the castings.

Characterization of Al/Fly ash composites

Mechanical characterizations

The tensile strength of the hybrid sample was measured at room temperature by using an Instron-4208 Universal Testing Machine (UTM). The ASTM standard E8M-09 was followed to prepare cylindrical cross-section tensile test specimens. Each specimen was prepared for monolithic pure aluminum as well as an Al/Fly ash reinforced composite. The tensile strength results were taken based on the average results obtained from three sample experimentations. Micro hardness tests were conducted by using the Brinell micro hardness instrument. To evaluate the reinforcement distribution in the matrix material, the hardness values are measured by applying a uniform indentation load at five different places on every sample. It is important to measure energy absorption nature of any metal which preferred to use as industrial counterpart. In this way the proposed hybrid samples tested for its low velocity energy absorption (Izod testing). The values of energy absorption rates were displayed for the discussion. The energy absorption in the neat samples and composite samples were used to measure the toughness property of the samples. It's also necessary to evaluate the ductile or brittle characteristics of the neat and hybrid composite samples in order to understand its internal strain energy towards impact loads.

Wear performance study

The Pin on Disc wear apparatus was used to conduct a wear test. The wear test was conducted at room temperature under dry sliding conditions according to the ASTM G99-04A standard. Initially, the specimen was polished and the burrs were removed by hand with an emery sheet. The pin size of 8 mm dia and a length of 30 mm were used for wear apparatus. The wear test

was carried out by constant values of sliding at a distance of 1200 m with a force of 20 N and a sliding speed of 500 rpm. The wear rate and coefficient of friction values were observed.

Microstructure analysis

Information about the materials' microstructure at the nano scale was captured using scanning electron microscopy. Primary, secondary, and back-scattered images produce grey scale images at the highest magnifications. Electrons, which are involved with the electron-matter interface, exhibit more information on the sample microstructure. Generally, backscattered electrons and secondary electrons provide topographical and atomic details, respectively, whereas diffused electrons represent the inner structure and crystallography. In this research, the morphology of the unfractured and fractured surface mechanisms was properly captured using SEM.

Results and Discussion

Morphology of the hybrid composites

Figure 1 represents the EDAX image of the 20 wt.% fly ash filled composites where there is a clear visibility in the carbon and oxide particles. Elements present in the samples with respect to the matrix and filler bonding were thoroughly studied and reported to indicate the existence of oxide and carbon particles in the matrix with moderate dispersion levels. Different kinds of signals were produced by electron beam-matter interaction that transmits various information about the specimen gets iteration 3 times each.

Figure 2 represents the different magnifications of the comparison of matrix filler bonding strength and dispersion level identification. It was noticed that the images have a significant number of pores and voids in the fly ash filled composition along with the agglomeration of the particles.

Tensile Test

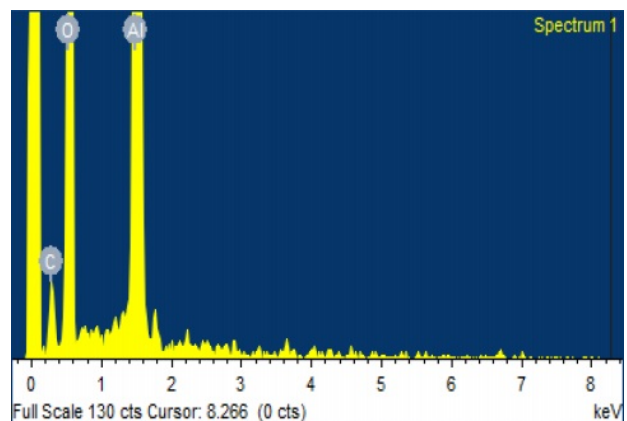


Fig. 1. EDAX - analysis of 20 wt.% fly ash filled samples.

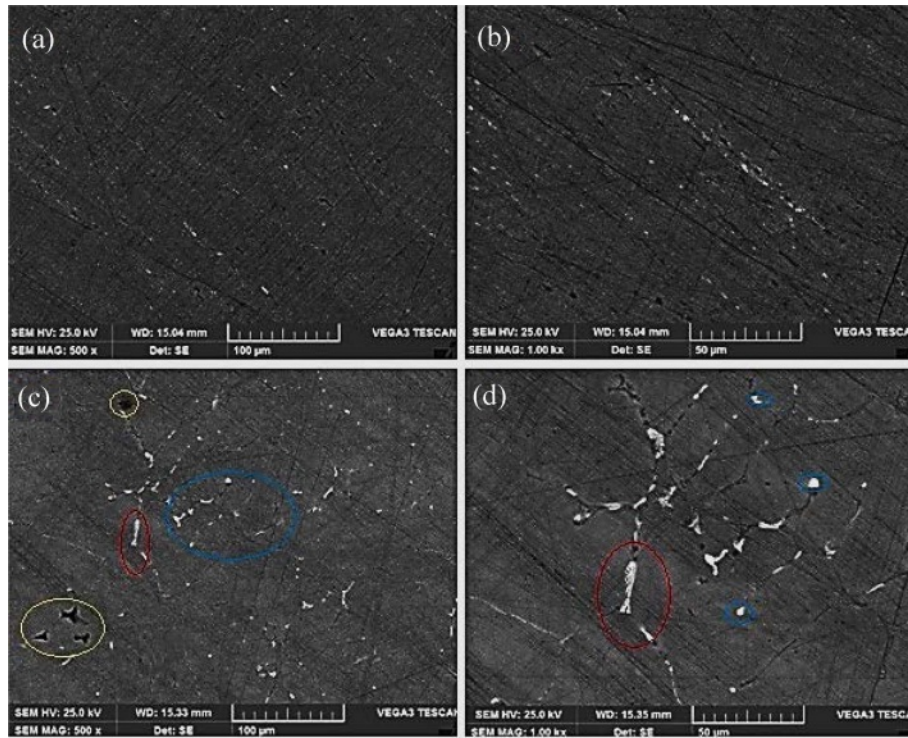


Fig. 2. SEM images of pure aluminium samples (a, b) and HC5 (c, d).

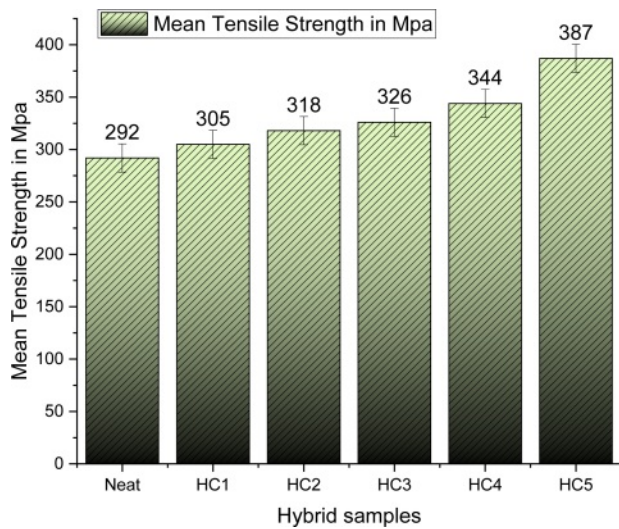


Fig. 3. Mean tensile strength comparison of pure and hybrid samples.

The variation of tensile strength and yield strength values by the influence of fly ash reinforcement content is shown in Fig. 3. The improvement of ductility and yield strength were based on the synthesis technique and the percentage of reinforcements. In ceramic reinforcements, the ductility was improved by grain refinements, texture modification, and non-basal slip systems. Three samples of each configuration were put through the tensile test, and the average values were found and shown. The yield strength is mainly enhanced by the homogeneous distribution of rein-

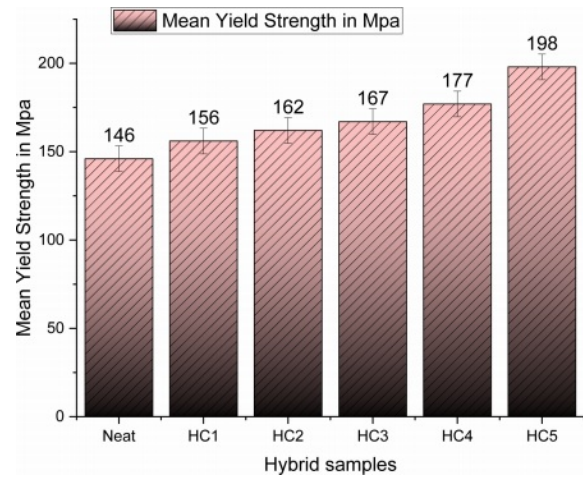


Fig. 4. Mean yield strength comparison of pure and hybrid samples.

forcements, grain refinement, and limited pores in the fly ash reinforced composites. The hybrid composite sample 5 has a higher tensile strength (35% increment) value when compared with pure aluminium, hybrid samples 2, 3 and 4. Fig. 4 shows the gradual increase in tensile strength up to sample 5. Results clearly show that there is a huge strength variation between pure aluminium samples and other hybrid samples (almost 40% higher than the base material). The average ultimate tensile strength of the cast composite is 387 MPa, which is significantly increased by up to 30% from the pure AA7075 aluminium matrix. The mean yield strength of the cast composite is about 198 MPa,

which is 29% higher than the pure AA7075. The main reasons for the strength improvement are homogenous particle distribution and interfacial bonding between fillers and matrix, which offer maximum strength when compared to other feeding samples. Fly ash composites with added fly ash improve energy absorption capacity and tensile loading effect in composite materials.

Micro Hardness

Addition of fly ash reinforcements clearly shows greater improvement in micro hardness values of hybrid composite samples as shown in Fig. 5. Neat laminates have a BHN of 57.1, whereas HC1, HC2, HC3, HC4, and HC5 have BHNs of 62.5, 65.32, 69.54, 76.02, and 82.45, respectively. Among all hybrid configurations, HC5 has an improved hardness value of 43.8% when compared with neat aluminium samples. The improvement of hardness values is due to the equal dispersion of fly ash reinforcement. Hardness

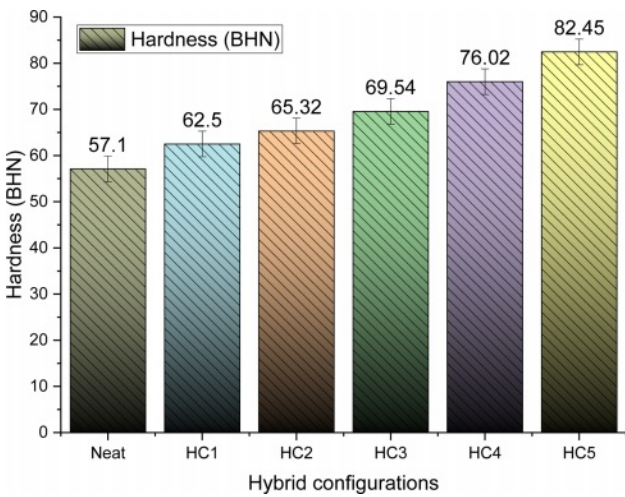


Fig. 5. Micro hardness results of the hybrid composites.

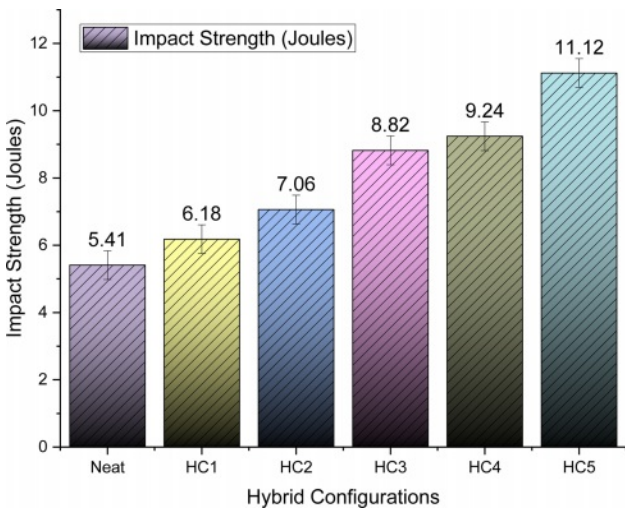


Fig. 6. Energy absorption behaviors of fabricated hybrid composites.

results were taken by a three-times average result of indentation in the Brinells hardness test. The same effects are observed in Al 2219/SiCp-Gr composites where the improvement of hardness value with an increasing percentage of reinforcements.

Impact strength

The energy absorption results of the samples are presented in Fig. 6. Neat laminates exhibit 5.41 joules of energy absorption, whereas HC1, HC2, HC3, HC4 and HC5 exhibit 6.18 joules, 7.06 joules, 8.82 joules, 9.24 joules, and 11.12 joules, respectively. It was observed from the results that the inclusion of fillers into the metal matrix gradually improves the energy management of the hybrid samples. Higher energy absorption can be obtained by enhancing the filler percentage. HC5 shows a higher energy absorption capacity of 11.12 joules, which is a remarkable value when compared with a neat aluminium sample. A gradual increase in the energy absorption indicates that

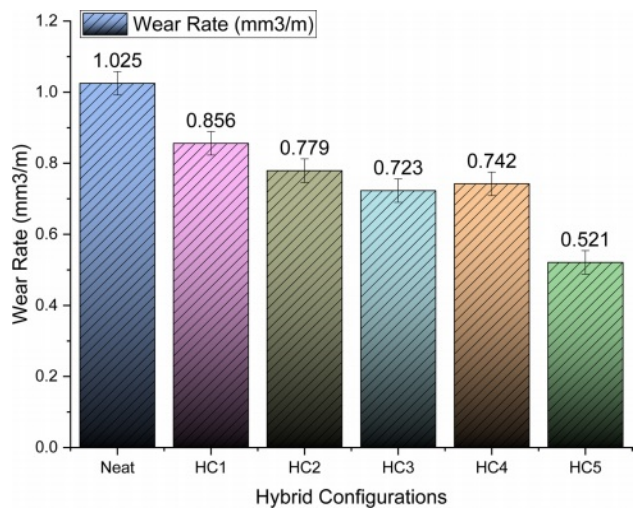


Fig. 7. Wear Rate of comparison of hybrid samples.

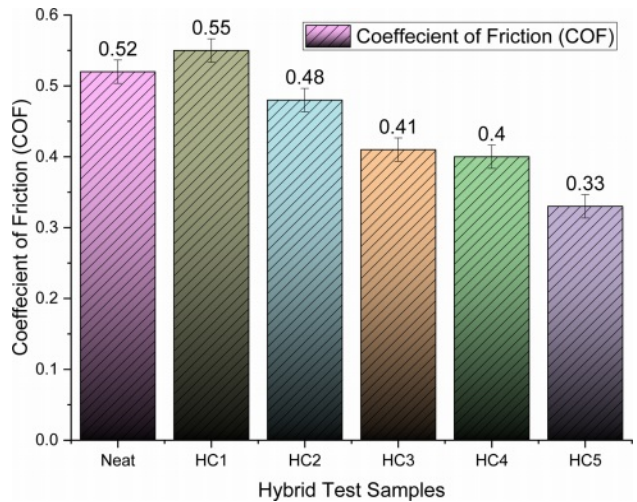


Fig. 8. Coefficient of friction of hybrid samples.

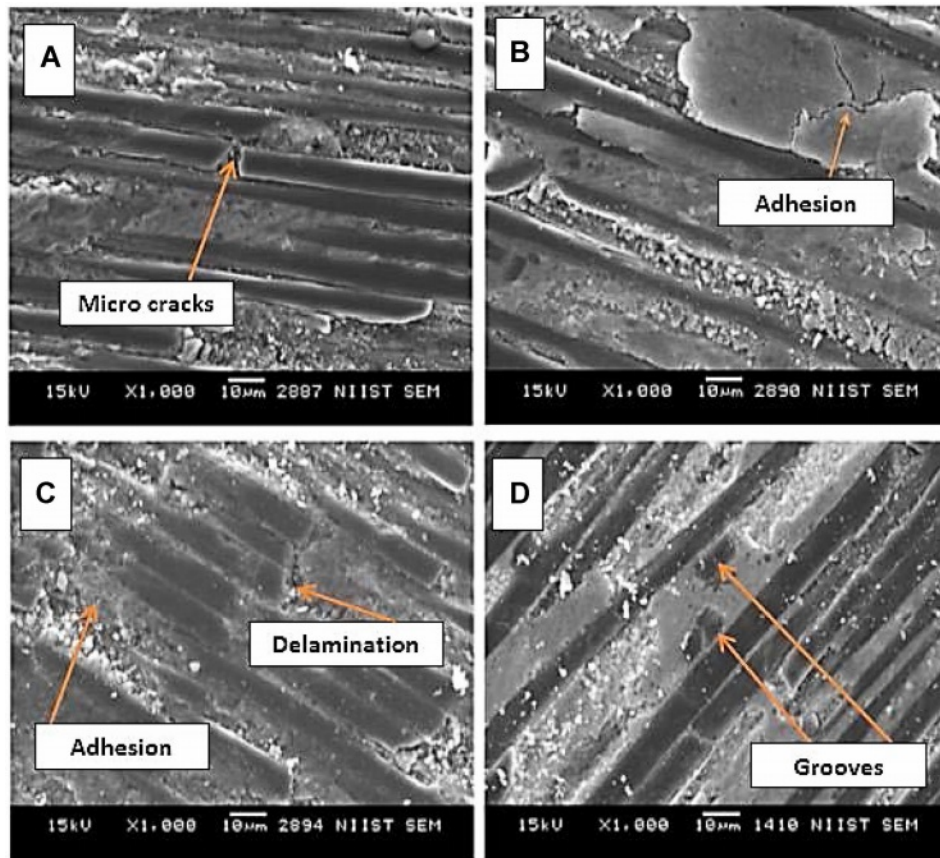


Fig. 9. Worn surface SEM study of hybrid samples (HC5).

there is a better filler arrangement in the matrix which transfers absorbed energy between them.

Sliding wear behaviour

The wear test of the proposed samples was conducted at a temperature of 25 °C and the relative humidity is about 50%. Initially, process parameters were varied such as load (1N, 1.5N, 2N, 2.5N, 3N), speed (up to 1000 rpm), with a constant time of 60 minutes for each testing cycle. The results clearly indicate that wear rates and coefficient of friction values were decreased with the increasing weight percentage of fly ash as shown in Figs. 7 and 8.

The remarkable 56% reduction in wear rate between neat aluminium and HC5. Similarly, the reduction percentage of wear rate was 13 and 30%, respectively, for samples HC2 and HC3 when compared with neat samples. The reduced wear rate is correlated with increased hardness values according to the Archard's wear law of an inverse relationship between wear rate and hardness. The friction coefficient of the hybrid samples gradually decreases with respect to the increase in the filler weight percentages. However, as for the wear rate of the samples, 20 wt.% fly ash filled samples outperform all similar grade samples.

Scanning Electron microscope

The microstructure of worn wear surfaces hybrid aluminium composites fabricated by using the stir casting method is shown in Fig. 9, where interfacial reaction and oxidation occurred during the casting of neat aluminium as displayed in Fig. 9(A).

Figure 9(A)-(D) depict the worn surfaces of highly reinforced fly ash sample-6 (HC5) images. The worn surfaces represent that the adhesive wear occurs on the unreinforced aluminium samples. The most important characteristics, such as groove pattern and abrasive wear, were clearly found in the worn surface SEM images. The craters were created due to applied load and plowing action on the surfaces of unreinforced magnesium samples. The wear rates were reduced by the addition of fly ash reinforcements in the samples. The increased load carrying capacity was observed and the reduced wear rate on the HC-5 samples has been shown in Fig. 9(D). From Fig. 9(D) worn surface images, it was observed that smaller craters and grooves evidenced that fly ash fillers improved load carrying capacity and reduced wear rate. The SEM images show that fly ash is homogeneously well distributed in the aluminium matrix composite.

Conclusion

In this proposed research, neat aluminium and fly ash (4, 8, 12, 16, 20 wt.%) composites were successfully produced by the stir casting method and the effects of mechanical properties, wear behaviour on their microstructures were compared between neat aluminium and hybrid composite samples. In this study, it has been noticed that the wear rate differs based on the applied load. Similarly, the gradual increase in tensile and hardness values was seen in the hybrid samples with respect to the increase in fly ash percentage. The wear rate and coefficient of friction are also reduced by the increased weight percentage of fly ash reinforcement. Weight loss rises normally with the increase in applied load. The reason behind the rise in wear rate is the plastic deformity at the tip of the sample surface asperity. The presence of fly ash was beneficial in reducing the wear rates and coefficient of friction. SEM images show that interfacial reactions occurred in fly ash particles during the casting process. As a result, reduced wear rates and improved mechanical properties favor developed Al/fly ash hybrid composites for wear resistant applications.

References

1. P. Bagde, S.G. Sapate, R.K. Khatirkar, and N. Vashishtha, *Tribol. Int.* 121 (2018) 353-372.
2. D. Aakash and M.K. Jain, *Recent Res. Sci. Technol.* 6 (2014) 30-35.
3. E. Thostenson, C. Li, and T. Chou, *Composites Sci. Technol.* 65 (2005) 491-516.
4. R. Karunanithi, Supriya Bera, and K.S. Ghosh, *Mater. Sci. Eng. B* 190 (2014) 133-143.
5. H. Fallahdoost, H. Khorsand, R. Eslami-Farsani, and E. Ganjeh, *Mater. Des.* 57 (2014) 60-68.
6. S. Natarajan, R. Narayanasamy, S.P. Kumaresh Babu, G. Dinesh, B. Anil Kumar, and K. Sivaprasad, *Mater. Des.* 30 (2009) 2521-2531.
7. Hani Ameen, *Am. J. Sci. Res.* 2 (2011) 99-106.
8. H.N. Reddappa, K.R. Suresh, and H.B. Niranjana, *Int. J. Appl. Res.* 2 (2011) 502-511.
9. K. Umanath, S.T. Selvamani, and K. Palanikumar, *Int. J. Eng. Sci. Technol.* 3 (2011) 5441-5451.
10. A.K. Mishra, V. Kumar, and R.K. Srivastava, *National Conference on Manufacturing Innovation Strategies & Appealing Advancements MISAA*, 2 (2014) 48278.
11. Ashok Kr Mishra et al., *J. Miner. Mater. Char. Eng.* (2014) 2351-2361.
12. Natarajan, S. et al., *Mater. Des.* (2009) 302521-302531.
13. J. Babu Rao, D. Venkata Rao, I. Narasimha Murthy, and N.R.M.R. Bhargava, *J. Int. J. Compos. Mater.* 46 (2012) 1393-1404.
14. K.M. Shorowordi, T. Laoui, A.S.M.A. Haseeb, J.P. Celis, and L. Froyen, *J. Mater. Process. Technol.* 142 (2003) 738-743.
15. B. Suresh Babu, G. Chandramohan, C. Boopathi, T. Pridhar, and R. Srinivasan, *J. Ceram. Process. Res.* 19[1] (2018) 69-74.
16. K.-H. Lin, K.-L. Wang, and Y.-T. Tsai, *J. Ceram. Process. Res.* 21[1] (2020) 103-112.
17. S.M. Soa, H.W. Hwang, S.H. Yia, J.S. Park, K.H. Kim, K.H. Lee, J. Park, and S.G. Lee, *J. Ceram. Process. Res.* 21[S1] (2020) S16-S22.